Journal of Materials Chemistry

Cite this: J. Mater. Chem., 2011, 21, 17810

www.rsc.org/materials

PAPER

Enhanced supercapacitors from hierarchical carbon nanotube and nanohorn architectures†

Pritesh Hiralal,*[ab] Haolan Wang,[a] Husnu Emrah Unalan,[c] Yinglin Liu,[b] Markku Rouvala,[b] Di Wei,[b] Piers Andrew[b] and Gehan A. J. Amaratunga[a]

Received 15th May 2011, Accepted 19th August 2011
DOI: 10.1039/c1jm12156a

Supercapacitors fill the power and energy gap between electrolytic capacitors and batteries. The energy density for commercial supercapacitors is currently limited to ~5 Wh kg^{-1}. Enhancing the energy and power density of supercapacitors is of great interest as it would open up a much wider range of applications. In this work, thin film supercapacitors made of random networks of single-walled carbon nanotubes (SWNTs) were enhanced by the use of carbon nanoparticles of a size ideal to fill the pores in the SWNT network. These nanoparticles, termed carbon nanohorns (CNHs), provide a much enhanced surface area, whilst maintaining high permeability and porosity. We demonstrate the hierarchical use of carbon nanostructures in a controlled fashion, allowing an enhancement provided by both types of materials, high power density by the SWNTs and high energy density from the CNHs. SWNT films serve as an ideal template onto which CNHs are deposited, with a good size match, adhesion and charge transfer between particles of a single chemical species. This combination results in an enhanced specific capacitance and a reduced equivalent series resistance (ESR) compared to a capacitor made of either individual component. Additionally, the good binding properties of the hybrid material and the high electrical conductivity of the SWNTs permit the removal of both the binder and the charge collector, paving the way for thinner and lighter supercapacitors. These electrodes allow the fabrication of supercapacitors with novel properties. As an example, we demonstrate a semitransparent supercapacitor. These results demonstrate the possibilities that may be available for the enhancement of electrodes by tailoring and combining relevant materials hierarchically in multiple scales. Much potential remains in further enhancement through tailored hierarchical nanostructuring.

1. Introduction

Energy storage technology has developed at a fast rate in the last few decades. The principal portable energy storage devices are broadly divided into three types: batteries, electrochemical capacitors (ECs) and dielectric capacitors, ordered in increasing power density and decreasing energy density. Batteries have high energy densities (up to 180 Wh kg^{-1}) and low power densities (up to 1 kW kg^{-1}).[1] ECs, also called supercapacitors, can deliver very high power densities (~15 kW kg^{-1}) with a lower stored energy than batteries (~5 Wh kg^{-1}).[2] These characteristics originate from the different mechanisms of energy storage in these devices. Supercapacitors are more appropriate for applications where high power is needed for a short period of time.[3] They also provide a good complement to Li-ion batteries in applications where both high energy (Li-ion batteries) and high power bursts (ECs) are required. The combination reduces the operational voltage dip at the load, extending energy efficiency and lifetime of the battery. An example of such an application would be powering the LED camera flash commonly used in mobile phones.

ECs have a number of other advantages as compared to batteries: lower equivalent series resistance (ESR), lower safety hazard and much longer cycle lifetimes. This comes as a result of the electrostatic charge storage mechanism, which does not involve any chemical reaction with the bulk of the electrode, removing bulk volume expansion strains on the electrodes, resulting in charge/discharge cyclabilities one or two orders of magnitude larger than for typical batteries. It also means that typically a faradaic efficiency (discharge time per charge time) of close to 100% is achieved. Given the fewer constraints in these devices, they can also be easily be adapted to work at low temperatures (~−40 °C) where batteries are not suitable. Currently, ECs provide an intermediate function between electrolytic capacitors and batteries in terms of energy and power

[a]Centre of Advanced Photonics and Electronics, Department of Engineering, University of Cambridge, 9 J. J. Thomson Ave., CB3 0FA Cambridge, UK. E-mail: pv237@cam.ac.uk; Tel: +44 01223 748 326
[b]Nokia Research Center, Broers Building, 21 J.J. Thomson Ave., CB3 0FF Cambridge, UK. E-mail: pritesh.hiralal@nokia.com
[c]Department of Metallurgical and Materials Engineering, Middle East Technical University, Ankara, Turkey

† Electronic supplementary information (ESI) available. See DOI: 10.1039/c1jm12156a

densities. However, given the advantages of supercapacitors, increasing their energy density to open up the avenue for more applications, even substituting batteries in some cases, is a very attractive prospect.

There are two common accepted charge storage mechanisms which lead to ECs. In electrochemical double layer capacitors (EDLCs), a purely electrostatic attraction occurs between the ions accumulated at the electrode/electrolyte interface, and the resulting double layer is the origin of the capacitance. This is the mechanism relevant for carbon-based electrodes. The second type of electrochemical capacitor, pseudo-capacitors, uses fast and reversible surface, or near-surface reactions for charge storage.[4] Electrode materials exhibiting pseudo-capacitance properties are generally metal oxides such as RuO_2[5] and MnO_2[6] or conducting polymers.[7,8] The large capacitance of ECs is a result of two main factors. Firstly, the formation of the Helmholtz double layer at the electrode/electrolyte interface results in a very short distance ($\sim$0.5 nm) between opposing charges and hence, a high capacitance. Secondly, materials typically used as electrodes have a very high surface area (in the range $\sim$1000 $m^2 g^{-1}$) on which this double layer can form.[9] Unfortunately, there is no simple relationship between the electrode surface area and the resulting capacitance.[10] Recent discoveries related to ion adsorption in carbon with pores in the nanometre range indicate that a careful control of pore size, structure and distribution is required for higher performing supercapacitors.[11] The advent of novel nanomaterials and the structure and size control achievable in these structures opens up many possibilities for engineering enhanced supercapacitor electrodes.

Due to their large surface area, many nanomaterials have been studied as candidates for supercapacitor electrodes. Carbon nanostructures are natural candidates due to their high electrical conductivity and electrochemical stability. As such, carbon fabrics, fibres, nanotubes, onions, nanohorns and nanoporous carbon derived from carbide[11] have been studied for supercapacitor applications. Structures like carbon nanotubes (CNTs), essentially graphene sheets rolled up to form highly conducting seamless cylindrical tubes, allow the flexibility of arrangement into various architectures which optimise different functions. For instance, they can be grown directly as aligned forests on charge collectors to optimise charge transport, or sprayed as random thin films to simplify deposition and allow a roll-to-roll process.[12,13] CNT-based supercapacitors have achieved very high power densities,[14] owing to their high conductivity; however, their energy density has as yet remained comparatively low. In addition, reported performances vary greatly due to the large effect of the quality and surface functionalisation of the CNTs.

A hybrid approach has been attempted in the last few years, whereby CNTs are used as a high surface area, highly electrically conducting scaffold onto which pseudo-capacitive materials are deposited, enhancing the capacitance of the CNTs and overcoming the intrinsically low conductivity that is common in pseudo-capacitive materials. This has been done with a number of nanoparticles including manganese oxide (MnO_2),[6] iron oxide (Fe_2O_3),[15] indium oxide (InO_2)[16] and polymer matrices.[17] However, capacitors fabricated from inorganic pseudocapacitive materials typically suffer from higher internal resistance and lower lifetimes.[18]

In this work we report on a double layer based hybrid capacitor electrode, based on a hierarchical combination of single-walled carbon nanotubes (SWNTs) and carbon nanohorns (CNHs). The combination results in an enhancement of energy density and lowering of internal resistance. The structure uses the fibrous SWNT network as both a capacitive element and a highly conducting charge collecting scaffold, onto which the CNHs are dispersed. CNHs are graphene sheets which have an origami-like contortion giving a conical horn-like shape typically 1–4 nm wide which typically agglomerate into 50–100 nm diameter particles. They are promising for energy conversion and storage devices[19] due to their high surface area, porosity and permeability. They can be easily prepared with high purity, at low cost and in large volumes.[20] This fully carbon-based hybrid system has the benefit of electrochemical stability, and good adhesion of the CNH to the template, removing the need of any binder. The high electrical conductivity of the SWNT[13,21] allows the possibility of constructing devices without a separate charge collector (albeit with a sacrifice in ESR). This leads to the possibility of energy storage devices with a much higher proportion of active material weight and allows the possibility of novel properties including transparency and flexibility. Additionally, an excellent charge transfer is expected between the different carbon materials. By combining the strengths of both materials in a hierarchical structure, an improved specific capacitance is obtained as compared to any of them used individually.

2. Experimental section

SWNT thin film preparation

SWNT thin films were deposited onto polyethylene terephthalate (PET) or glass substrates by a vacuum filtration method as described in detail elsewhere.[22] Briefly, purified and –COOH functionalized SWNTs (Nanocyl 1101, 90+% C purity) were dispersed in deionized water containing 1 wt% sodium dodecyl sulfate (SDS). The resulting solution was then vacuum filtered onto mixed cellulose ester (MCE) membranes (pore size 0.22 μm) and the surfactant was washed away with copious amount of deionised water. The films were transferred onto substrates through a short annealing process followed by selective dissolution of the membrane in consecutive acetone and isopropanol washings. The resulting film consists of consolidated SWNTs on substrates bonded by intimate van der Waals contact. The SWNT solution concentration was 2 mg l^{-1} and the filtration volume was varied to change the film density, from 20 to 80 ml. The resulting films were circular with a 2 cm^2 area. The sheet resistance of the SWNT thin films varied from 3.1 kΩ sq^{-1} to 200 Ω sq^{-1}, depending on SWNT density, corresponding to transparency values ranging from 60% to 20%, respectively.

CNH synthesis

CNHs were produced by arc discharge in liquid nitrogen using graphite anodes and cathodes which were 3 and 12 mm in diameter, respectively. Full details of the process are described elsewhere.[20] An arc current of 60 A was used. At the end of the discharge process, CNHs were collected, dried, and subsequently dispersed in deionised water and drop cast onto the SWNT thin

films. Typically, 0.07 mg of CNH was dispersed onto a SWNT film.

Supercapacitor fabrication

Once the electrodes were ready, a small strip of palladium was sputtered as charge collector from the edge of the CNT film to the edge of the PET, onto which an Al foil was attached with silver dag for convenient external contact.

A mixed ester cellulose paper was used as a separator. It was soaked in 1 M sulfuric acid (H_2SO_4) and sandwiched in between two carbon electrodes (Fig. 2). The supercapacitor was then sealed with Scotch tape and used as prepared. For the transparent version, Nafion film was used as a transparent separator.

Characterisation

The morphology of the fabricated samples was determined by a combination of scanning electron microscopy (JEOL 6340F, operated at 5 kV) and scanning tunnelling electron microscopy (Hitachi S5500 STEM, operating at 30 kV). The specific surface area of the materials was determined by Brunauer–Emmett–Teller (BET) nitrogen adsorption (Micromeritics). Electrochemical properties of the capacitor were studied in two electrode form with a fully formed device, and were measured with a potentiostat/galvanostat (Autolab PGSTAT 302N). Optical absorption measurements were made using a Thermoelectron Corporation UV/Vis Spectrometer UV2 double beam spectrophotometer.

3. Results and discussion

SWNT thin films were deposited onto PET substrates by the vacuum filtration method. A scanning electron microscope (SEM) image of a SWNT thin film uniformly covering the PET substrate surface is shown in Fig. 1(a). Pore sizes of the film range from a few tens of nm to a few hundreds of nm. Water dispersions of CNHs were drop-cast onto the SWNT film. An SEM image of CNHs partially covering the SWNT film is shown in Fig. 1(b). The CNH nanocarbon powder consists of agglomerates of CNHs (<100 nm particle size) with pore sizes of 0.427 nm. Fig. 1(c) shows a high magnification STEM image of a CNH aggregate, where individual protruding horn-shaped nanostructures are visible. Horn openings are typically 3–5 nm in width while tips have a radius of curvature of 1–2 nm. The nanocarbon powder provides a very large surface area (~1025 $m^2\ g^{-1}$) and high porosity for increased energy storage. Fig. 1(d) shows the nitrogen adsorption measurements of SWNTs and CNHs. The enhancement provided by the CNHs can be clearly observed. Exposure to the electrolyte and anchorage to the substrate electrode are facilitated by the SWNT template. CNHs form a free powder. Unless a binder is used, adhesion to each other or to the surface is very poor. Enhanced surface binding of CNHs onto SWNTs may be observed by eye. Hybrid SWNT/CNH films suffered no visible variation in texture or conductivity after 1000 bending cycles with a ~7 mm bend radius.

The as-deposited carbon electrodes were packaged into two terminal devices (Fig. 2) and their electrochemical properties were measured immediately after fabrication.

Cyclic voltammograms of supercapacitors based on solely SWNT thin films of varying thickness are shown in Fig. 3(a). Film thickness is dependent on the volume of CNT solution filtrated. Thicknesses are quoted in the figure, however, they are only indicative figures, due to the highly porous nature of the films which make a precise value unreliable. Thicker films were found to be more conducting, and as expected, showed a higher capacitance. These measurements were made at a scan rate of 20 mV s^{-1}. The capacitance increases from 2.0 mF cm^{-2} for a 40 ml filtrated SWNT solution to 3.9 mF cm^{-2} for an 80 ml solution. The slope deviating from the ideal capacitor shape is a result of the internal resistance of the devices,[4] which remains relatively high compared to that of similar devices with a metal current collector. The curves also show small current peaks which we ascribe to stray pseudocapacitance resulting from the functional groups of the SWNTs or from residual surfactant remaining from the thin film preparation process. The specific

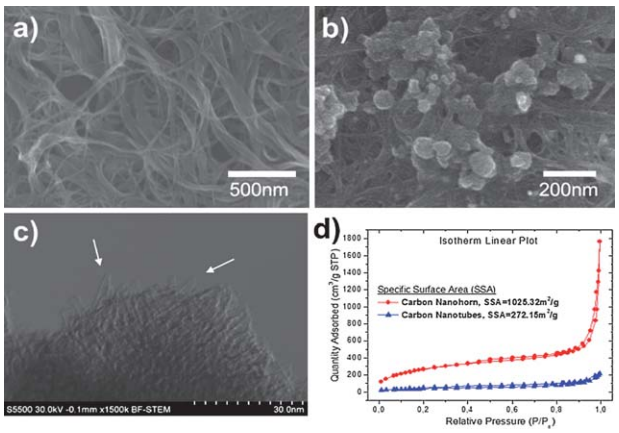

Fig. 1 Scanning electron micrographs of (a) a typical SWNT thin film and (b) a SWNT thin film partially coated with CNHs. (c) High magnification STEM image of CNH agglomerates taken in TEM mode. Arrows indicate individual nanohorns protruding out of the aggregation of CNHs. (d) N_2 adsorption isotherm plots for SWNT and CNH, showing the comparative surface area of both types of nanocarbons.

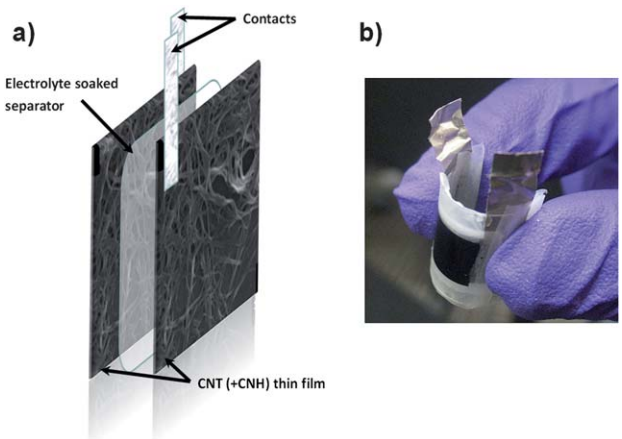

Fig. 2 (a) Schematic of the supercapacitor structure. (b) Photograph of a flexible supercapacitor constructed on a PET substrate.

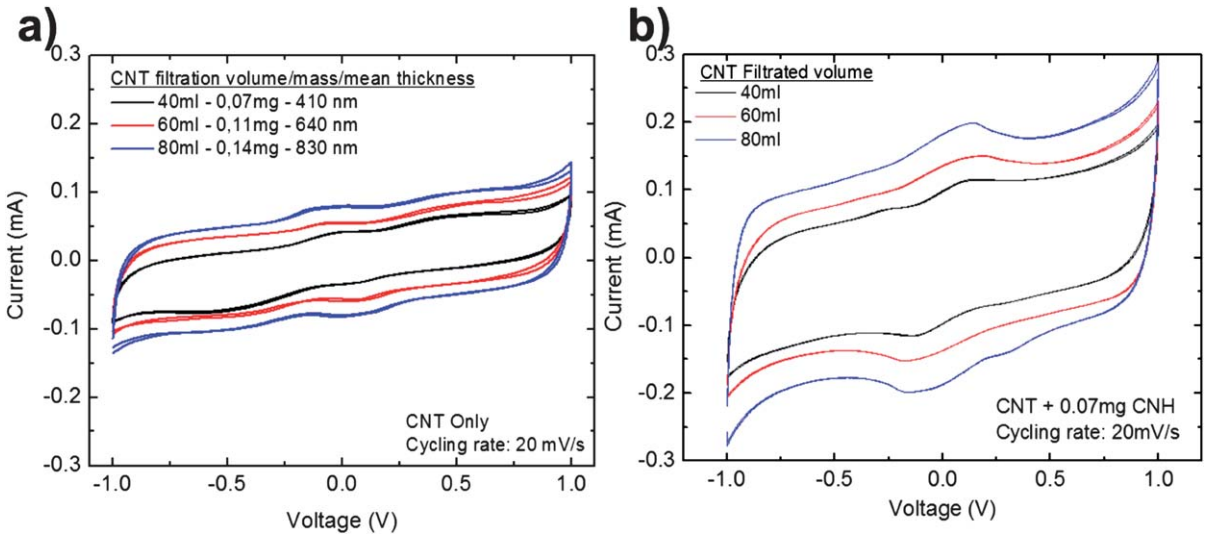

Fig. 3 Cyclic voltammograms of (a) CNT thin film electrodes of different thicknesses produced using different volumes of vacuum filtration. (b) The same CNT films with a constant 0.07 mg of CNH added. The scan rate is 20 mV s^{-1}.

capacitance of these electrodes is about 28 F g^{-1} and decreases slightly with increasing electrode thickness. The capacitance was calculated using the relation $C = I/(dV/dt)$ at the zero potential point, where I is the current (averaged from charge and discharge values) and dV/dt is the scan rate.

The slight decrease in specific capacitance (F g^{-1}) with increasing film thickness (despite the increase in capacitance per area) is expected, as increasing SWNT thickness results in a reduced overall permeability and hence it becomes more difficult for the electrolyte to access the active area at the base of the electrode. This reduction in permeability is compensated to some extent by increased film conductivity.

The discharge profiles of the electrodes above are shown in Fig. 4(a). Upon addition of 0.07 mg of CNHs onto the matrix,

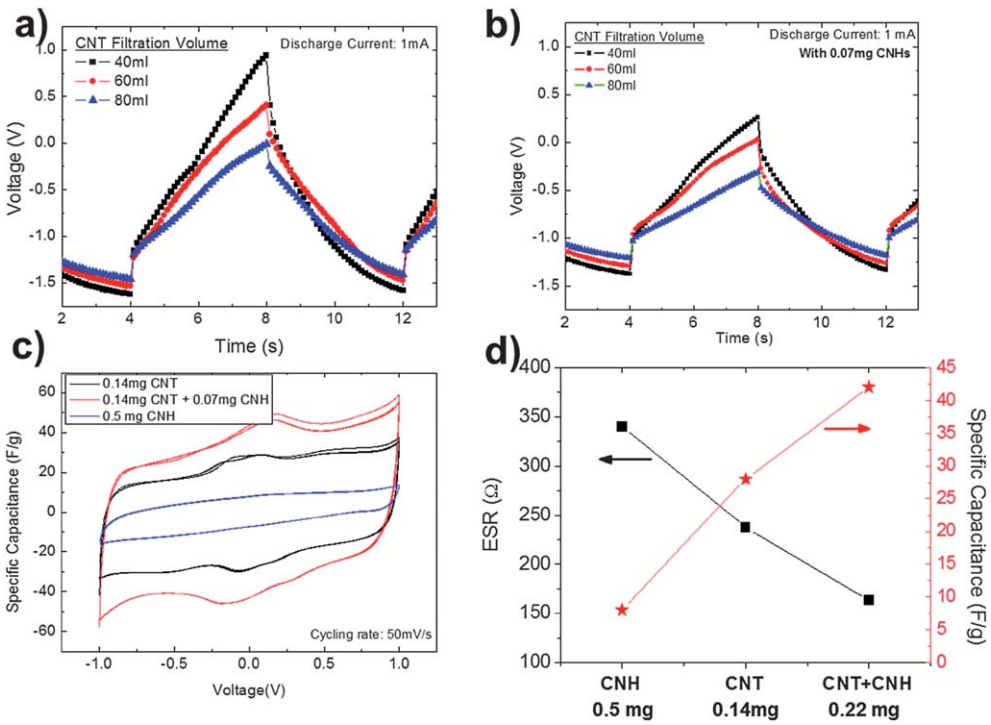

Fig. 4 (a) Discharge profile of SWNT thin film supercapacitors. (b) Discharge profile of the same devices upon addition of 0.07 mg of CNH. (c) Cyclic voltammograms showing the specific capacitance of CNH, SWNT and the combination of both. (d) Diagram showing the change in equivalent series resistance (ESR) and specific capacitance with the different material combinations.

the capacitance increases significantly. Fig. 4(b) shows the discharge characteristic of the SWNT + CNH combination. The enhancement is somewhat disproportionate to the increase in active material weight. Fig. 4(c) shows cyclic voltammograms normalised with respect to mass for 3 different electrodes, all of which act as both the charge collector and active material. Despite their very high surface area (~1025 m^2 g^{-1}), CNHs by themselves show poor capacitance due to poor particle adhesion, resulting in poor interparticle charge transport. No charge collector or binder was used, in order to fully demonstrate the advantage of the hybrid structure. The combination of materials in a hierarchical fashion benefits from the advantages of both, and results in the highest capacitance per area and weight. These results are summarised in Fig. 4(d).

Capacitors made solely of SWNT thin films have been reported before.[13] There are several approaches for making these films, from vacuum filtration[12,23] to spraying.[13] The resulting films have been reported to contain pores of two length scales, 1–10 nm and 10–100 nm,[24] the first is ascribed to the internal pores of tubes and bundles, whilst the latter is ascribed to the larger pores which form as a result of the morphology of the film. These latter pores provide large non-active volumes for capacitance but are of ideal size for fitting CNH aggregates.

Typical surface areas of SWNT thin films are not too high (350–450 m^2 g^{-1})[24] due to the tubes' packing format, which conspires to obstruct the porosity in such films, restricting the accessible surface area.[23] CNHs, on the other hand, offer a high specific surface area (~1025 m^2 g^{-1}) as obtained from nitrogen physisorption tests; however, partly due to their particulate nature and poor interparticle adhesion, they have a poor charge transport. Intercalation of CNHs in the pores of the SWNT thin films allows for a vast increase in surface area. We also found that films were stable upon drying without the addition of any additional binder, and that the CNHs attached well to the SWNTs, allowing for an enhanced charge collection.

The combination offers an enhanced specific capacitance which was maintained up to the electrode weights which we tested. This improvement is likely to be associated with the much higher porosity (75%) of CNHs, a high intrusion pore volume (6.3 ml g^{-1} as measured by mercury porosimetry) and a very high permeability (5100 mDarcy), substantially higher than typical activated carbons, combined with the high conductivity of the CNTs. Additionally, given the graphitic nature of both materials, it is reasonable to expect good interparticle charge transfer characteristics, and hence a reduction in ESR. A summary of the different properties of the capacitors with different material combinations is shown in Table 1.

Specific energy and power densities are calculated from:

$$E_{sp} = \frac{1}{2} \times \frac{CV^2}{m} \quad (1)$$

$$P_{sp} = \frac{V^2}{4 \times \mathrm{ESR} \times m} \quad (2)$$

where E_{sp} and P_{sp} are energy and power densities, respectively, C is the capacitance of the device, m is the total mass of the active material, and V is the maximum voltage with the electrolyte used (*i.e.* 1 V). The limited power density is a result of the high ESR resulting from the poor conductivity of the thin SWNT films and the high contact resistance with the external contact. We estimate that a metal current collector would in this case bring power densities up to >250 kW kg^{-1} (only taking active material into account). Using this structure, and although our SWNT thin films have not been optimised to obtain the highest transparency to conductivity ratios (60% transmittance at 550 nm for 3.1 kΩ sq^{-1} *vs.* 75% transmittance at ~100 Ω sq^{-1} (ref. 25)), it is possible to demonstrate the concept of a flexible supercapacitor with some degree of transparency. Fig. 5 shows the performance of a supercapacitor for which all components (PET/SWNT thin film/separator/electrolyte) exhibit some degree of transparency. The cyclic voltammogram (Fig. 5(a)) shows about a 20 F g^{-1} specific capacitance, albeit with very high ESR, for this device. The combined transparency of all layers is about 23% at 550 nm (Fig. 5(d)), however most of the absorption comes from the unoptimised SWNT films (Fig. 5(c)). We expect optimisation of the current device to allow for the fabrication of supercapacitors of capacitances of a few mF cm^{-2} and a transparency of >60%.

Table 1 Summary of the typical performance characteristics of supercapacitors made of the different carbon nanomaterials

	Mass/mg	ESR/Ω	Power density/kW kg^{-1}	Energy density/Wh kg^{-1}
CNT	0.14	238	3.63	3.94
CNH	0.5	340	0.74	1.08
CNT + CNH	0.22	163	3.50	6.03

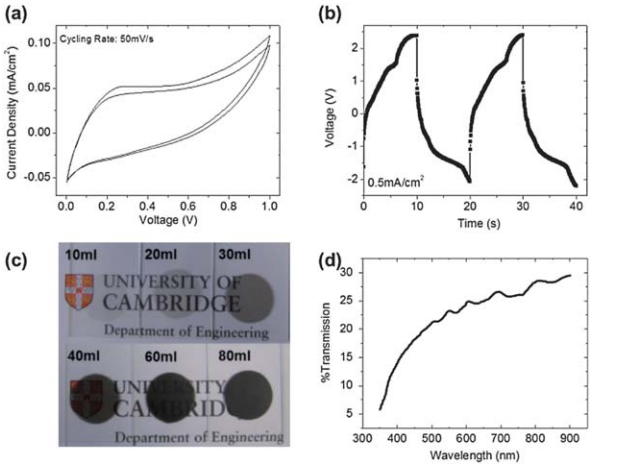

Fig. 5 Semi-transparent supercapacitor (a) cyclic voltammogram and (b) charge/discharge characteristic taken at a constant 0.5 mA cm^{-2}. (c) Photograph of CNT thin films of different thicknesses on glass. (d) Optical transmission characteristics of the full device.

Conclusions

Overall, we see that a controlled architecture allows design of electrodes with pore sizes over various length scales, resulting in improved capacitor characteristics. This hybrid structure opens up new possibilities in electrode design. The hierarchical structure allows the advantages of each material to be exploited. CNHs provide a cheap, mass manufacturable, high surface area and high permeability electrode material, while the SWNT thin

films provide a highly conductive, porous network with very good physical binding to the CNHs, removing the need for an additional binder. The integration of functionalities also allows the production of thicker electrodes without a reduction in specific capacitance *i.e.* maintenance of good electrolyte permeability without any loss in charge transport. Additionally, the need for a separate charge collector is removed, due to the conductive nature of the film, aiding to reduce the overall mass. The possibility of a carbon based pure EDLC device which shows some degree of transparency is demonstrated for the first time. However, deposition on a metallic foil would aid reduction of the overall ESR. The deposition method for both materials is low cost, occurs at low temperature and is readily scalable. Enhanced fabrication methods which allow a much better interpenetration of the two particles are underway. Given the low cost fabrication method of the CNHs, and the small amount of SWNTs used, the hybrid structure may also allow a more economic use of otherwise expensive CNTs in supercapacitors.

Acknowledgements

This work was supported under the Nokia-Cambridge Strategic Alliance in Nanoscience and Nanotechnology.

References

1 P. Simon and Y. Gogotsi, *Philos. Trans. R. Soc. London, Ser. A*, 2010, **368**, 3457–3467.
2 B. E. Conway, *Electrochemical Supercapacitors: Scientific Fundamentals and Technological Applications*, Springer, 1999.
3 J. R. Miller and P. Simon, *Science*, 2008, **321**, 651–652.
4 E. Frackowiak, *Carbon*, 2001, **39**, 937–950.
5 J. M. Miller and B. Dunn, *Langmuir*, 1999, **15**, 799–806.
6 H. Zhang, G. Cao, Z. Wang, Y. Yang, Z. Shi and Z. Gu, *Nano Lett.*, 2008, **8**, 2664–2668.
7 A. Laforgue, *J. Power Sources*, 1999, **80**, 142–148.
8 M. Mastragostino, *Solid State Ionics*, 2002, **148**, 493–498.
9 P. Simon and Y. Gogotsi, *Nat. Mater.*, 2008, **7**, 845–854.
10 O. Barbieri, M. Hahn, A. Herzog and R. Kotz, *Carbon*, 2005, **43**, 1303–1310.
11 J. Chmiola, G. Yushin, Y. Gogotsi, C. Portet, P. Simon and P. L. Taberna, *Science*, 2006, **313**, 1760–1763.
12 M. Kaempgen, C. K. Chan, Y. Cui and G. Gruner, *Nano Lett.*, 2009, **9**, 1872–1876.
13 M. Kaempgen, J. Ma, G. Gruner, G. Wee and S. G. Mhaisalkar, *Appl. Phys. Lett.*, 2007, **90**, 264104.
14 C. Du and N. Pan, *Nanotechnology*, 2006, **17**, 5314–5318.
15 X. Zhao, C. Johnston and P. S. Grant, *J. Mater. Chem.*, 2009, **19**, 8755.
16 P.-C. Chen, G. Shen, S. Sukcharoenchoke and C. Zhou, *Appl. Phys. Lett.*, 2009, **94**, 043113.
17 M. Hughes, G. Z. Chen, M. S. P. Shaffer, D. J. Fray and A. H. Windle, *Chem. Mater.*, 2002, **14**, 1610–1613.
18 N.-L. N. Wu and S. L. Kuo, *Investigation on Cycling Stability of Mn-Containing Oxide Supercapacitors*, ECS, 2007, vol. 3, pp. 11–15.
19 C.-M. Yang, Y.-J. Kim, M. Endo, H. Kanoh, M. Yudasaka, S. Iijima and K. Kaneko, *J. Am. Chem. Soc.*, 2007, **129**, 20–21.
20 H. Wang, M. Chhowalla, N. Sano, S. Jia and G. A. J. Amaratunga, *Nanotechnology*, 2004, **15**, 546–550.
21 A. Jorio, M. Dresselhaus and G. Dresselhaus, *Carbon Nanotubes: Advanced Topics in Synthesis, Structure, Properties and Applications*, Springer-Verlag, Berlin, Heidelberg, 2008.
22 H. E. Unalan, G. Fanchini, A. Kanwal, A. D. Pasquier and M. Chhowalla, *Nano Lett.*, 2006, **6**, 677–682.
23 R. K. Das, B. Liu, J. R. Reynolds and A. G. Rinzler, *Nano Lett.*, 2009, **9**, 677–683.
24 S. M. Cooper, H. F. Chuang, M. Cinke, B. A. Cruden and M. Meyyappan, *Nano Lett.*, 2003, **3**, 189–192.
25 S. B. Yang, B.-S. Kong, D.-H. Jung, Y.-K. Baek, C.-S. Han, S.-K. Oh and H.-T. Jung, *Nanoscale*, 2011, **3**, 1361–1373.